

# Effect of PWHT cycles on fatigue crack growth and toughness of quenched and tempered pressure vessel steels

Z. Sterjovski<sup>a,\*</sup>, D.G. Carr<sup>b</sup>, D.P. Dunne<sup>a</sup>, S. Ambrose<sup>c</sup>

<sup>a</sup> Faculty of Engineering, University of Wollongong, Northfields Avenue, NSW 2522, Australia

<sup>b</sup> Materials Division, Australian Nuclear Science and Technology Organisation, PMB 1, Menai 2234, Australia

<sup>c</sup> Welding Technology Institute of Australia (WTIA), Silverwater, NSW 2128, Australia

## Abstract

Transportable pressure vessels, commonly manufactured from quenched and tempered (QT) steels, require mandatory postweld heat treatment (PWHT) regardless of plate thickness. During their life, transportable pressure vessels may have up to 4 PWHT cycles at temperatures between 540 and 590 °C, and concerns have emerged about possible effects on the mechanical properties of the base (parent) plate.

This paper reports work on the resistance to fatigue crack growth, impact toughness and CTOD fracture toughness of two types of QT steels. The parent metal region was examined for both steels, and then exposed to temperatures and times in the PWHT range. Although there was a marginal decrease in the resistance to fatigue crack growth for up to four postweld heat treatment cycles, there was a significant decrease in impact toughness and CTOD fracture toughness.

© 2004-Elsevier B.V. All rights reserved.

**Keywords:** Postweld heat treatment; Quenched and tempered steel; CTOD; Impact toughness; Void coalescence; Fatigue crack growth; Transportable pressure vessels

## 1. Introduction

Postweld heat treatment (PWHT) is a mandatory and costly step in the manufacture or weld repair of transportable pressure vessels fabricated from quenched and tempered (QT) steel. PWHT is a stress relieving process whereby residual stresses are reduced in QT steels by heating between 540 and 590 °C for a set time depending upon plate thickness. There have been limited reports [1–8] that the stress relieving process can lead to adverse effects on the toughness and/or fatigue properties of the base plate, especially when repeated or multiple PWHT cycles are applied. Some previous reports [8,9] suggest that although PWHT deleteriously affects toughness [8], there is little effect on fatigue crack growth.

All reported cases (approximately 10) of accidents involving transportable pressure vessels in Australia show that catastrophic failure (failure that penetrates through thickness and causes leakage) occurred only in the parent plate [1]. One reported accident, which occurred in October 1995, involved a tanker manufactured from ATSM A517 QT steel. The tanker had a shell thickness of 10 mm and a head thickness of 6 mm. The tanker, which had a PWHT history of 30 min holding time at 570 °C, was deformed by 900 mm to a partly concave shape (Fig. 1(a)), and the plate was folded ~150° to give three folds meeting at one point, where a crack penetrated through the head wall (Fig. 1(b)). The crack site was more than 100 mm from any weld [10]. This observation is consistent with reports that conclude that the impact properties of simulated coarse-grained heat affected zone and weld metal structures are superior to the base plate, even with increased heat treatment time [7].

PWHT in transportable pressure vessels is currently mandatory for all plates, whereas non-transportable pressure

\* Corresponding author. Tel.: +61 2 42214842.

E-mail address: zoran@uow.edu.au (Z. Sterjovski).

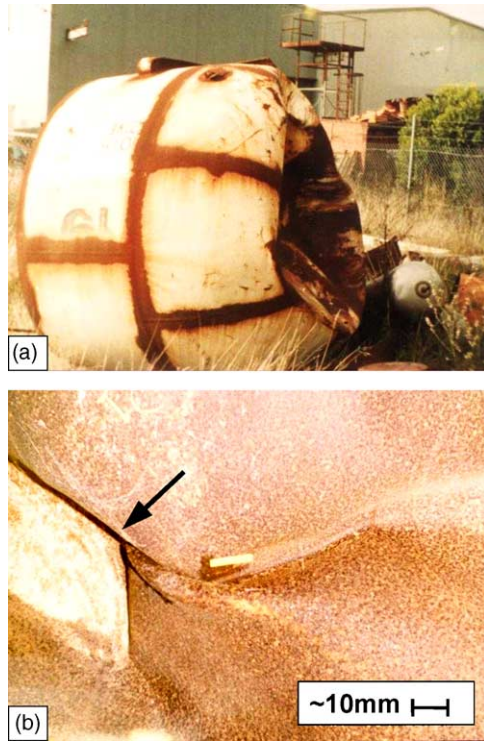


Fig. 1. (a) Front head of QT steel tanker following a high velocity collision and (b) a penetrating crack formed in the PM region resulting from the high velocity collision [10].

vessels only require PWHT for QT steel plates greater than 15 mm in thickness [11]. This requirement, as well as the fact that Australian Standards do not quantify the effects of elevated temperatures and cumulative holding times on material properties, led to the initiation of this project.

BIS80PV (11 mm), a QT pressure vessel steel, was selected with the aim of accumulating data to show the effect of PWHT cycles or cumulative holding time on toughness and fatigue crack growth rates. BIS80 (12 mm) was also tested because it has higher impact toughness than BIS80PV and is considered a possible pressure vessel material.

Rolling direction and microstructural banding are influential in the fracture of the parent metal (PM), and so, impact and CTOD samples were oriented with the length of the sample transverse to the direction of rolling and the notch in the direction of rolling. Scanning electron microscopy (SEM) was used to evaluate the effect of multiple PWHT cycles on fracture mode.

## 2. Experimental methods

### 2.1. Materials selection

Quenched and tempered steel was selected for an Australian Research Council funded project titled, "Optimisation of PWHT in Transportable Pressure Vessel Steels" because of its widespread use in the transportable pressure vessel in-

Table 1  
Chemical compositions (wt.%)

	11 mm	12 mm		11 mm	12 mm
C	0.1700	0.1550	Al	0.0310	0.0040
P	0.0110	0.0100	Sn	<0.002	0.0050
Mn	1.4300	1.1000	Nb	<0.001	<0.001
Si	0.2000	0.1900	Ti	0.0250	0.0260
S	0.0035	0.0030	V	0.0030	<0.003
Ni	0.0290	0.0200	B	0.0005	0.0013
Cr	0.2000	0.0160	Ca	0.0008	0.0008
Mo	0.2100	0.2100	N	0.0031	0.0033
Cu	0.0110	0.0090	O	0.0020	0.0022

dustry in Australia. Bisalloy Steels Pty Ltd provided QT steel plate in thicknesses typically used for transportable pressure vessels (11- and 12-mm).

The 11-mm plate is classified as BIS80PV (pressure vessel plate) in accordance with AS3597-1993 [12]. The 12-mm BIS80 plate is QT structural plate and considered a possible candidate for pressure vessels. The measured compositions of the plates are shown in Table 1.

### 2.2. Heat treatment

Postweld heat treatment of all samples was carried out in a box furnace. Heat treatment conformed to AS4458-1997-Pressure Equipment Manufacture, and was conducted in an argon atmosphere.

The temperature of treatment was  $570 \pm 5$  °C (validated by two thermocouples attached to each plate), and the holding time was 30 min. The ramp up rate was 200 °C/h and samples were then cooled in still air. Up to 4 PWHT cycles were applied because this is the maximum number of cycles a transportable pressure vessel would normally be expected to undergo during its service life.

### 2.3. Fatigue testing—crack growth rates

Fatigue crack propagation data were collected on standard CTOD samples exposed to various PWHT cycles. These samples required fatigue pre-cracking at room temperature for subsequent CTOD testing. Fatigue pre-cracking was carried out at a frequency of 30 Hz and an *R*-ratio (minimum fatigue load:maximum fatigue load) of 0.1. Table 2 quantifies the loads used for fatigue pre-cracking.

The fatigue crack length,  $a_i$ , was estimated using the compliance method described in ASTM E1820 [13]. This involved a series of loads/unloads and corresponding clip gauge displacement measurements to determine the crack length after every 1000 cycles. The crack growth rate,  $da/dN$ , was

Table 2  
Fatigue cycle loads (kN)

	Maximum load	Minimum load	Mean load	Amplitude
11 mm	8.12	0.81	4.47	3.66
12 mm	9.50	0.95	5.23	4.28

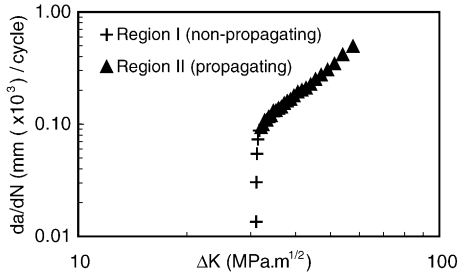


Fig. 2. Typical plot of  $da/dN$  (log scale) vs.  $\Delta K$  (log scale) for pressure vessel grade QT steel.

calculated every 1000 cycles until a desired fatigue crack length was achieved for CTOD testing.

The stress intensity factor range,  $\Delta K$ , was calculated from the loads in Table 2 to obtain a plot of  $da/dN$  versus  $\Delta K$  (Fig. 2).

$$\Delta K = K_{\max} - K_{\min} \quad (1)$$

$$K_{\max \text{ OR } \min} = \frac{P_{\max \text{ OR } \min} S}{BW^{3/2}} f\left(\frac{a}{W}\right) \quad (2)$$

where  $P_{\max}$  is the maximum fatigue load (N),  $P_{\min}$  is the minimum fatigue load (N),  $B$  is plate thickness (m),  $S$  (m) and  $W$  (m) are defined in Fig. 3 and  $f(a/W)$  is defined in ASTM E1290 [14].

The triangular data points (correspond to Region II [15]) in Fig. 2 were modelled by Eq. (3), in which  $n$  is the slope of the curve (Paris Law) [15].

$$\frac{da}{dN} = C \Delta K^n \quad (3)$$

where  $n$  and  $C$  are material constants.

#### 2.4. Fracture toughness testing—CTOD

CTOD fracture toughness was carried out on plates exposed to 0, 2 and 4 PWHT cycles. The samples were full plate thickness and taken transverse to the direction of rolling (with the notch in the direction of rolling). Testing was car-

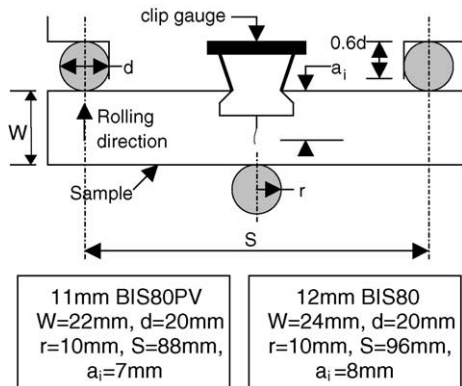


Fig. 3. Schematic representation of CTOD test set up.

ried out in accordance with ASTM E1290-99 using the SE(B) specimen geometry [14].

The test temperature selected was  $-20^\circ\text{C}$  and a ramp rate of 1 mm/min was used. The specimen was set up as shown schematically in Fig. 3.

Post-test procedure involved physical measurement of the fatigue pre-crack length and the amount of slow stable crack extension. There are three subscripts that may be assigned to the CTOD,  $\delta$ , namely [14]:

1.  $\delta_c$ —is given at the onset of unstable brittle crack extension or pop in when the final crack length less the original crack length ( $\Delta a_p$ ) is less than 0.2 mm.
2.  $\delta_u$ —is given at the onset of unstable brittle crack extension or pop in when  $\Delta a_p$  is greater than 0.2 mm.
3.  $\delta_m$ —is given at the attainment of a maximum force plateau for fully plastic behaviour.

The material exhibited size-dependent fully plastic behaviour and the following equation for  $\delta$  was used to calculate  $\delta_m$  at the attainment of maximum load [14]:

$$\delta = \frac{K^2(1 - \nu^2)}{2\sigma_{YS}E} + \frac{r_p(W - a_0)\nu_p}{r_p(W - a_0) + a_0 + z} \quad (4)$$

where  $K$  is defined by Eq. (2),  $\nu_p$ , 0.33;  $r_p$ , 0.44;  $\nu_p$ , plastic component of clip gauge opening displacement;  $\sigma_{YS}$ , yield or 0.2% proof stress; and  $z$ , 0.

Averages of the CTOD values were taken (from 3 to 5 samples) and plotted versus the number of PWHT cycles.

#### 2.5. Impact testing—Charpy V-notch

Impact testing was carried out in accordance with AS1544-1989. A striking energy of 325 J was used and the test temperature was  $-20^\circ\text{C}$  as required by the Australian Pressure Vessel and QT Steel Standards [12]. Averages of five samples were taken from each group of tests.

Samples were machined to AS1544.2-1989 (standard size) from the middle of the plate to assess impact energy where banding and segregation effects would be most severe. Impact test results are presented in the same orientation as the CTOD samples.

#### 2.6. Scanning electron microscopy

Scanning electron microscopy was used to study the fracture surfaces of Charpy V-notch and CTOD samples.

### 3. Results

#### 3.1. Fatigue crack growth rate

Fig. 4 shows the fatigue crack growth exponent,  $n$  (Eq. (3)), versus the number of PWHT cycles. It can be seen in Fig. 4 that the resistance to fatigue crack growth is lower in the

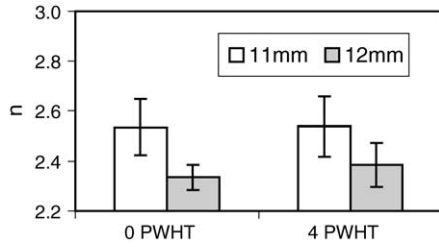


Fig. 4. Fatigue crack growth rate exponent,  $n$ , for 0 and 4 PWHT cycles. Error bars represent standard deviation.

11 mm BIS80PV ( $n=2.55$ ) than the 12 mm BIS80 ( $n=2.36$ ). Fig. 5 is a plot of  $da/dN$  versus  $\Delta K$  using experimentally determined  $n$  and  $C$  values (Eq. (3)). This figure confirms the superior resistance to fatigue crack growth of the 12-mm BIS80 plate over the 11-mm BIS80PV plate and it also shows the slight adverse effect of 4 PWHT cycles on resistance to fatigue crack growth.

3.2. CTOD fracture toughness

CTOD testing was selected as the most appropriate form of fracture toughness testing because of its relative simplicity and compatibility as a toughness measure to carry out fracture toughness assessments to BS-7910-1999—“Guide on methods for assessing flaws in metallic structures”. Fracture toughness testing focussed solely on the PM region because of the association with real-life failures in this region.

Fig. 6 plots CTOD (mm) versus the number of PWHT cycles for 11-mm BIS80PV and 12-mm BIS80. This figure shows that PWHT adversely affects fracture toughness. The subscript assigned to  $\delta$  is m, which implies that these samples failed with fully plastic behaviour [14]. Fig. 6 also shows that the CTOD of the 12-mm PM is superior to the 11-mm PM regardless of the number of PWHT cycles.

3.3. Charpy V-Notch impact toughness

Charpy V-notch impact testing was carried before PWHT and up to and including 4 PWHT cycles. This was the main

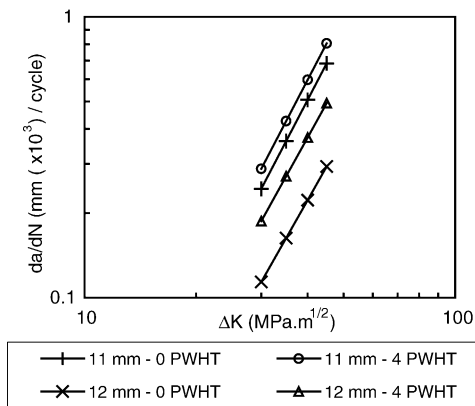


Fig. 5.  $da/dN$  (log scale) vs.  $\Delta K$  (log scale) for 0 and 4 PWHT cycles.

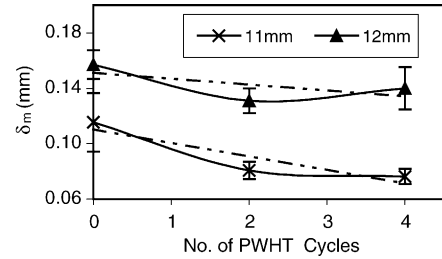


Fig. 6. CTOD (mm) at  $-20^{\circ}\text{C}$  vs. the number of PWHT cycles. Error bars represent standard deviation.

focus of the research as it is the failure of transportable pressure vessels at high velocity (high strain rate collisions) that is of major concern to the Australian pressure vessel industry. All results are from the T–L orientation because the lowest impact energy is given when the test sample runs transverse to the direction of rolling and the notch is in the direction of rolling.

Fig. 7 compares the impact energy values of 11-mm BIS80PV and 12-mm BIS80 plate versus the number of PWHT cycles. From this graph it is evident that as the number of PWHT cycles increases there is a decrease in impact energy. After 4 PWHT cycles the impact energy of the 11 mm T–L samples falls below 40J and does not satisfy the requirements of the Australian Pressure Vessel Standards [12]. Similarly, for 12-mm BIS80 samples, the deleterious consequence that heat treatment cycles have on impact energy is evident.

Fig. 7 also shows that the impact energy of 12-mm BIS80 is superior to 11-mm BIS80PV, regardless of the number of PWHT cycles.

3.4. SEM fractography

The fracture surfaces of CTOD samples were examined by SEM. Scanning electron fractographs were critical in this research, in that valuable information regarding the mechanism and nature of failure could be determined. SEM fractographs of CTOD samples of 12-mm plates exposed to 0, 2 and 4 PWHT cycles in the region near the

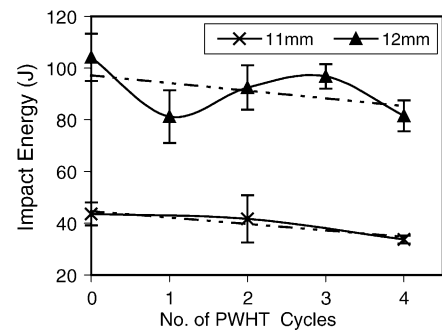
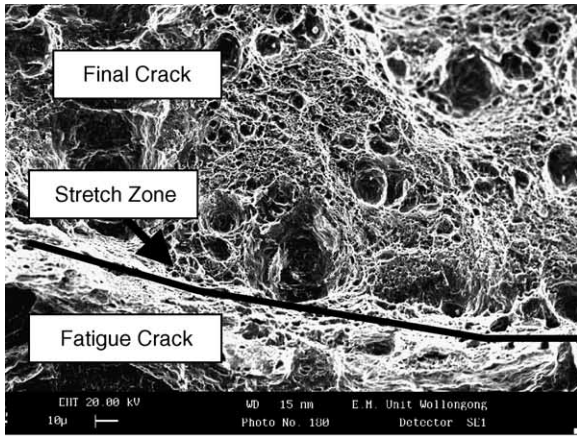
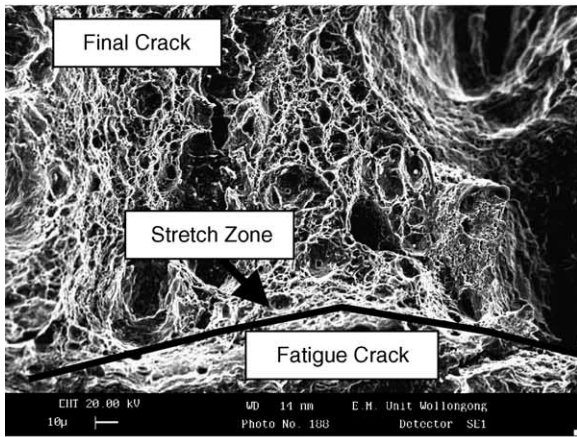


Fig. 7. Impact energy (J) at  $-20^{\circ}\text{C}$  vs. the number of PWHT cycles. Error bars represent standard deviation.

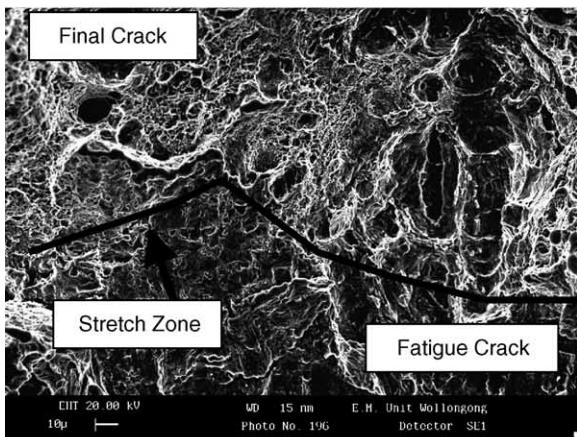
fatigue crack/final crack interface are shown in Fig. 8. Additionally, SEM fractographs of the general fracture area of 12 and 11 mm Charpy samples are respectively shown in Figs. 9 and 10.



(a)



(b)

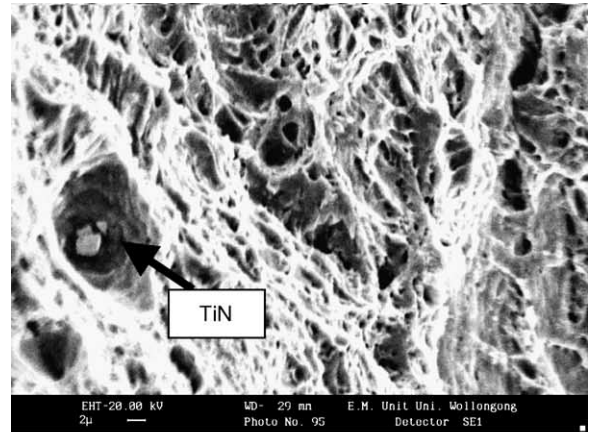


(c)

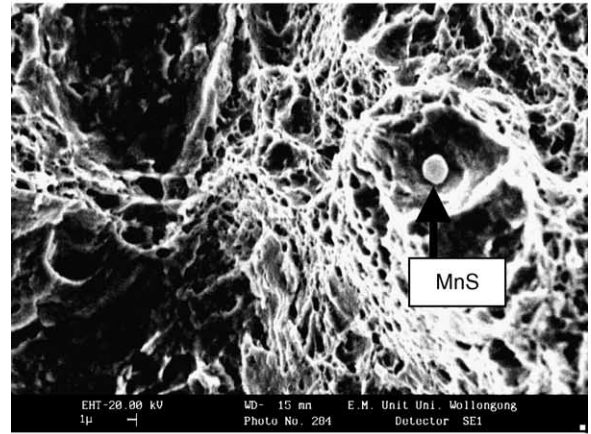
Fig. 8. Typical CTOD fracture surface images of the fatigue crack/final crack interface of 12-mm BIS80 exposed to (a) no PWHT; (b) 2 PWHT cycles; and (c) 4 PWHT cycles (10  $\mu$ m bar).

### 3.5. Comparison of CTOD fracture toughness and Charpy impact toughness

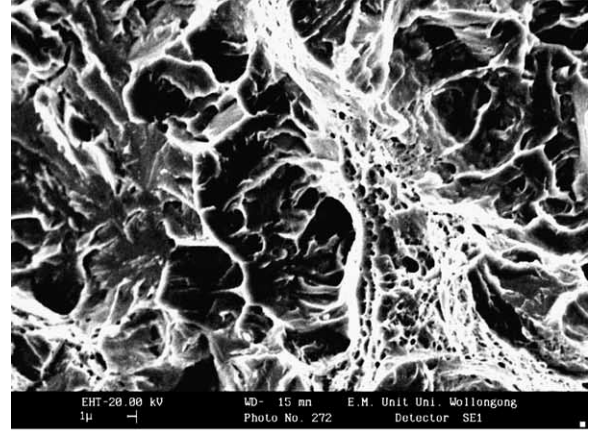
A sound correlation between CTOD fracture toughness and impact toughness could lead to considerable cost savings to industry in the area of design. The data in Fig. 11 indicate a general increase in impact energy with increas-



(a)

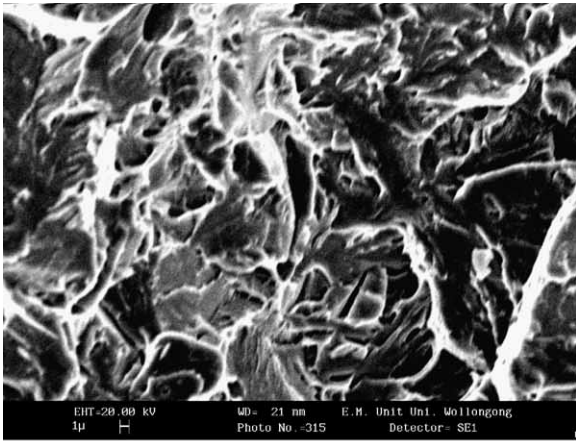


(b)

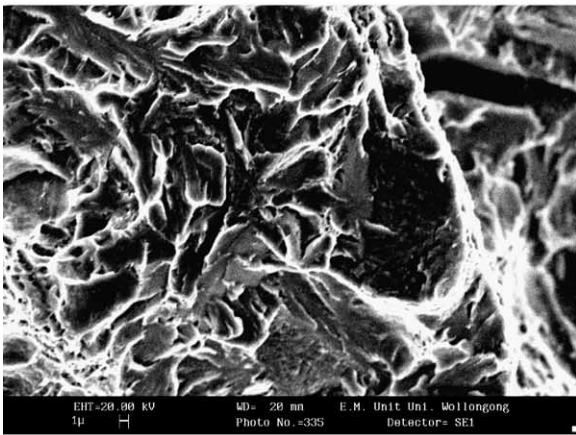


(c)

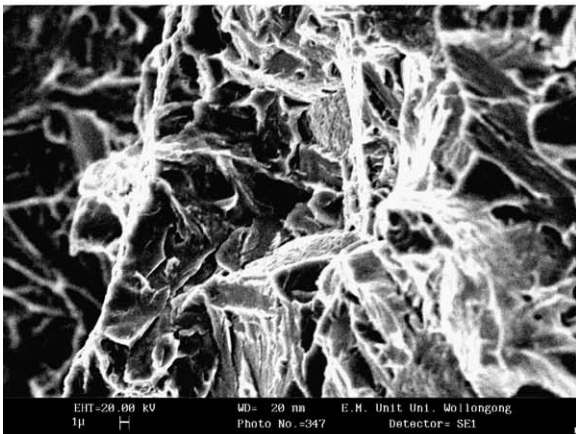
Fig. 9. Typical Charpy fracture surface images of the general fracture area of 12-mm BIS80 exposed to (a) no PWHT (2  $\mu$ m bar); (b) 2 PWHT cycles (1  $\mu$ m bar); and (c) 4 PWHT cycles (1  $\mu$ m bar).



(a)



(b)



(c)

Fig. 10. Typical Charpy fracture surface images of the general fracture area of 11 mm BIS80PV exposed to (a) no PWHT; (b) 2 PWHT cycles; and (c) 4 PWHT cycles (1  $\mu$ m bar).

ing CTOD values. Fig. 12 shows increasing CTOD values with a decrease in the ductile–brittle transition temperature (DBTT).

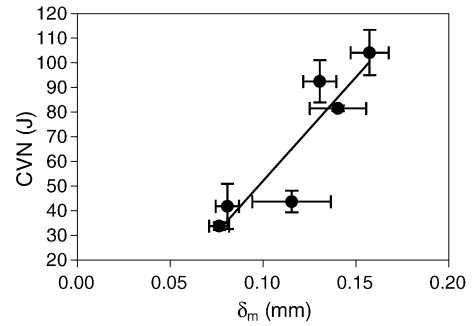


Fig. 11. Impact toughness at  $-20^\circ\text{C}$  vs. CTOD for 11- and 12-mm samples. Error bars represent standard deviation.

#### 4. Discussion

A major aim of the project was to investigate the effect of multiple PWHT cycles on the fatigue and toughness properties of the PM region of QT pressure vessel steels. The PM region is of paramount concern to the Australian pressure vessel industry because this is the zone reported to fail in traffic collisions. Further, PWHT cycles have been reported to be detrimental to the mechanical properties of the PM [1,7,8]. Transportable pressure vessels are exposed to multiple PWHT cycles because PWHT is mandatory in the repair or manufacture of these vessels. The heat treatment must be applied to the entire vessel and PWHT holding time is dependent on the maximum plate thickness of the walls of the pressure vessel.

The resistance to fatigue crack growth is important in transportable pressure vessels as they are exposed to cyclic loading in transit. Fatigue crack growth data were collected on CTOD samples exposed to 0 and 4 PWHT cycles. Fig. 4 shows that after 4 PWHT cycles there is a marginal increase in the fatigue crack growth rate for both BIS80 (12-mm) and BIS80PV (11-mm) QT steels. This trend can be clarified through the findings of Kwun and Fournelle [5] whose research shows that steels containing second phase carbides (Nb carbides) exhibit a faster fatigue crack growth rate than steels that do not. Hence, exposure to an increasing number of PWHT cycles results in the initiation, coarsening and

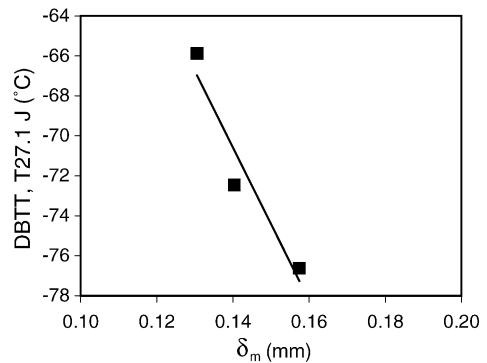


Fig. 12. DBTT ( $^\circ\text{C}$ ) vs. CTOD (mm) for 12-mm BIS80 samples.

coalescence of carbide particles, which in turn increase the rate of fatigue crack growth.

However, there are reports in the literature that state heat treatment has no effect on fatigue crack growth rate [7,8]. Two examples of this are Logsdon [8], who reported that fatigue strength was unaffected by heat treatment at 538 °C for 24 h and 607 °C for 24 or 48 h in A508 (Class 2a) and A533 (Grade B, Class 2) steels, and Horikawa et al. [9], who stated that PWHT had little effect on fatigue crack growth in the base plate of an HT80 steel (0.12 wt.% C, 0.88 wt.% Mn, 0.89 wt.% Cr, 0.31% Mo and 0.04% V). Figs. 4 and 5 also show the slightly greater resistance to fatigue crack growth of 12-mm BIS80 compared with 11-mm BIS80PV.

CTOD fracture toughness testing was carried out to examine the effect of multiple PWHT cycles on CTOD fracture toughness ( $\delta$ ). All samples showed a decrease in  $\delta$  as the number of PWHT cycles increased (see Fig. 6). SEM was used to examine and determine the mechanism by which PWHT leads to a decrease in  $\delta$ . Fig. 8 shows the fractographs of 12 mm CTOD samples exposed to 0, 2 and 4 PWHT cycles. Fig. 8(a), which has not been postweld heat-treated, shows predominantly void coalescence in the final crack region, which failed with stable crack growth. For 2 PWHT cycles, the size of the voids increased, as shown in the fractograph in Fig. 8(b). This is indicative of coarsening of second phase carbide particles that can still initiate ductile failure [20]. Further, exposure to 4 multiple PWHT cycles resulted in regions with even larger voids (see Fig. 8(c)). Similar trends were evident in the SEM fractographs of the CTOD of 11 mm BIS80PV exposed to 0, 2 and 4 PWHT cycles. Fig. 8(c) also shows a greater presence of cleavage fracture in the final crack region, which occurs in the presence of coarser second phase particles that are too large to initiate ductile failure.

In Fig. 7, which is a plot of impact energy versus number of PWHT cycles, it is evident that the impact energy of the PM decreases as the number of PWHT cycles is increased. This trend is more pronounced in 11-mm BIS80PV plate. After 4 PWHT cycles the 11-mm PM impact energy decreased from approximately 45 to 27 J and the 12-mm plate impact energy decreased from approximately 108 to 88 J.

Figs. 11 and 12 reflect the general trend of increasing CVN and decreasing DBBT (°C) with increasing CTOD ( $\delta_m$ ), but the correlation is based on limited data and more measurements would be needed to establish more quantitative correlations. Despite the limited number of data points, trends similar to those presented by Dolby [22] were evident, that is, an increase in the DBTT (°C) correlated with a decrease in CTOD fracture toughness.

As was found for resistance to fatigue crack growth, the impact toughness and CTOD toughness of 12-mm BIS80 is higher than 11-mm BIS80PV (Figs. 6 and 7). This is due to the difference in the chemical compositions of the two steels. The 12-mm BIS80 plate has significantly less carbon, manganese, sulphur and chromium, resulting in higher ductility. It is well known that increased levels of carbon and sulphur

produce more brittle steel [16]. Also, higher levels of manganese and chromium are reported to be associated with steels that exhibit splitting of fracture surfaces and lower energy failures (in impact testing) [17,18]. Moreover, sulphur combines with manganese to form elongated MnS particles (after rolling) that reportedly decrease resistance to crack propagation [19]. The superior CTOD fracture toughness of 12-mm BIS80 clarifies the greater resistance to fatigue crack growth of this steel over 11-mm BIS80PV plate.

SEM of the Charpy V-notch fracture surfaces was carried out to ascertain the mechanism by which increasing PWHT cycles resulted in decreasing the impact energy required to cause failure. SEM fractographs were of the general fracture area (away from splits and shear lips).

Fig. 9(a) shows an image of a relatively ductile fracture surface in the as-welded condition and Fig. 9(c) shows an image of a predominantly brittle fracture surface following 4 PWHT cycles. Therefore, it can be stated that the fracture appearance progressively becomes more brittle as the number of PWHT cycles increase.

Honeycombe and Bhadeshia [20] state that ductile fracture, in the form of void coalescence, initiates at fine second phase particles (most likely carbides). Fig. 9(a and b) are indicative of void coalescence and the mechanism involves the nucleation and growth of voids in the plastic zone ahead of the crack tip, thus, promoting fracture. In comparing Fig. 9(a and b), it is evident that the voids are smaller in diameter when there is no exposure to PWHT. Hence, it can be deduced that there should be very fine and dispersed second phase carbide particles throughout the matrix. As the second phase carbide particles coarsen, the voids increase in diameter and facilitate crack growth (Fig. 9(b)). Then when the second phase carbide particles reach a certain size by a growth-coalescence mechanism their ability to initiate voids is impaired [20] resulting in quasi-cleavage, a more brittle mode of cracking, at a lower impact energy (see Fig. 9(c)).

The effect of multiple PWHT cycles on the Charpy fracture surface of 11-mm BIS80PV is not as clear as 12-mm BIS80 because all the surfaces show quasi-cleavage fracture (Fig. 10). In the fractograph of the 11-mm sample without PWHT (Fig. 10(a)), a quasi cleavage brittle type fracture is evident in comparison to the ductile fracture of the corresponding 12-mm sample. The reason for this lies in the differences in the chemical composition of the two steels. The 11-mm BIS80PV plate contains more C, Mn, S and Cr, which are detrimental to impact toughness. There was a significant decrease in impact energy after 2 PWHT cycles and then 4 PWHT cycles, but visual comparison is difficult because all of the surfaces are predominantly cleavage fracture. It is proposed that the coarsening of existing carbides continues, which leads to a lower impact energy failure due to shearing of larger particles.

A review by Dunne [21] on the theoretical and experimental background of hydrogen assisted cold cracking in steel weldments, discusses the fracture modes of void coalescence and quasi cleavage fracture, and explains how coarser

second phase particles result in a lower impact energy and a more brittle fracture surface. In void coalescence, fine second phase particles cause fine voids to initiate ahead of the crack tip (transgranular fracture), hence propagating the fracture. As these precipitates coarsen, the voids formed ahead of the crack tip increase in size, and thus, the fracture propagates with less energy. In quasi-cleavage fracture, both transgranular fracture of the particles or intergranular fracture at the particle–matrix interface can occur, leading to localised cleavage fractures rather than void formation. The particles become fracture acceleration sites. This type of fracture requires the least amount of energy and has a shorter fracture path.

In summary, as PWHT cycles increase there is an increase in the diameter of the voids due to the coarsening of second phase carbide particles. Fig. 9(a and b), which respectively show large voids due to large TiN and MnS particles, lend support to the fact that void diameter is proportional to the second phase particle size (whether they are carbides, nitrides or sulphides).

Finally, as the number of PWHT cycles increases it is evident that a decrease occurs both in CTOD value and impact toughness (Figs. 6 and 7). The data in Fig. 11 do indicate a general increase in impact energy with increasing CTOD value, but a strong correlation is not evident. This result is consistent with a lack of reports in the literature of a strong correlation between these two properties.

## 5. Conclusions

Data from these tests and the corresponding analysis led to the following conclusions.

- Impact toughness of the PM decreased as the number of PWHT cycles or holding time was increased and there was a progressive change in the fracture appearance towards a more brittle fracture.
  - SEM fracture analysis of Charpy impact and CTOD samples is consistent with growth and coalescence of second phase carbide particles in the QT PM structure.
  - The fracture toughness and impact toughness of the 12-mm BIS80 plate was higher than that of the 11-mm BIS80PV because of a more favourable chemical composition.
  - The CTOD fracture toughness of 11-mm and 12-mm plate decreased with increasing number of PWHT cycles.
- Resistance to fatigue crack growth of the PM was marginally compromised following multiple PWHT cycles.

## Acknowledgements

The authors gratefully acknowledge the support of ANSTO, CRC for Welded Structures, Bisalloy Steels, WTIA–Panel 1 and 2, and CCI Pope.

## References

- [1] M.O. O'Brien, R.F. Lumb, *Australasian Weld. J.* 45 (2000) 45, third quarter.
- [2] C.C. Wang, Y. Chang, *Metall. Mater. Trans. A* 27A (October) (1996) 3162–3169.
- [3] P. Yongyuth, P.K. Ghosh, P.C. Gupta, A.K. Patwardhan, S. Prakash, *Int. J. Joining Mater.* 5 (March) (1993) 31–38.
- [4] G. Nicoletto, *Int. J. Press. Vessels Piping* 42 (3) (1990) 363–378.
- [5] S.I. Kwun, R.A. Fournelle, *Metall. Trans. A* 13A (March) (1982) 393–399.
- [6] A. Amirat, K. Chaoui, *J. Mater. Sci.* 38 (3) (2003) 575–580.
- [7] G. Pimenta, F. Bastian, *J. Mater. Eng. Perform.* 10 (2) (2000) 192–202.
- [8] W.A. Logsdon, *J. Mater. Energy Syst.* 3 (March) (1982) 39–50.
- [9] K. Horikawa, S. Fukuda, Y. Kishimoto, *Trans. JWRI* 10 (October) (1981) 219–231.
- [10] S. Ambrose, Highway accident with a quenched and tempered steel pressurised road tanker, 1992, Private report.
- [11] Australian Standard 4458, AS4458-1997 Pressure Equipment—Manufacture, 1997.
- [12] Australian Standard 3597, AS3597-1997 Structural and Pressure Vessel Steel—Quenched and Tempered Plate, 1997.
- [13] ASTM E1820, Standard Test Method for Measurement of Fracture Toughness, 2001.
- [14] ASTM E1290, Standard Test Method for CTOD Fracture Toughness Measurement, 1999.
- [15] G.E. Dieter, *Mechanical Metallurgy*, McGraw Hill, 1988.
- [16] G.M. Evans, N. Bailey, *Metallurgy of Basic Weld Metal*, Abington Publishing, 1997.
- [17] J.E. Ryall, J.G. Williams, *Fracture Surface Separations in the Charpy V-Notch Test*, BHP Technical Bulletin 22 November (2) 1978.
- [18] A.J. DeArdo, *Metall. Trans. A* 8A (1977) 473–486.
- [19] S.R. Yeomans, *Welding in Structural Engineering Steels and Aluminium Alloys*, School of Civil Engineering, University College, UNSW, Canberra, Australia, 1994.
- [20] R. Honeycombe, H. Bhadeshia, *Steels: Microstructures and Properties*, second ed., Edward Arnold, 1995.
- [21] D.P. Dunne, *Proceedings of the WTIA 47th Annual Conference*, 17–20 October, 1999.
- [22] R.E. Dolby, *Weld. Inst.* (1981) 1–6.